COBEM 2023 27TH INTERNATIONAL CONGRESS OF MECHANICAL ENGENEERING

ABCM Brazilian Society of Mechanical Sciences and Engineering
27th ABCM International Congress of Mechanical Engineering
December 04-08, 2023, Florianópolis-SC, Brazil

COBEM2023-2204
EFFECTS OF CANOPY ARCHITECTURE IN WIND-ENERGY POTENTIAL FOR POWER GENERATION BY WIND TURBINES

Mario B. B. Siqueira
Antonio C. P. Brasil Jr.
Universidade de Brasília
mariosiqueira@unb.br ; brasiljr@unb.br

Luis Aramis R. Pinheiro
Universidade de Brasília
aramisrp@gmail.com

Abstract. *Wind turbines are invariably inserted in a region of the atmosphere called the Atmospheric Boundary Layer (ABL), which is directly influenced by the presence of the Earth's surface and responds to surface forcings. As such, the ABL comprises the part of the troposphere closest to the surface with a vertical dimension of the order of 1km during the day. However, the lowermost layers of the ABL are directly affected by the geometry of the elements that constitute the surface roughness, such as trees in forests, the so-called roughness sub-layer, which can extend up to 4 heights of these elements. Therefore, as wind turbines have rotor heights close to 100m, besides being always in the ABL, depending on the surface cover where it is inserted, it might be under the effects of the vegetation architecture, i.e., canopy height and leaf area distribution, LAD. In this work, it was examined the effects of different vegetation covers on the potential for electrical power generation by wind turbines. Two types of vegetation were considered that are quite distinct in both their geometric and phenological characteristics, namely, native Cerrado and a Eucalyptus plantation. A one-dimensional (vertical) atmospheric flow model based on the solution of the Reynolds-averaged Navier-Stokes equations with second order closure, was developed for canopy flow, where its elements such as foliage, branches and trunks act as sinks for linear momentum. Dry and wet season simulations, characteristic of the Brazilian Centro-Oeste, with corresponding LAD for each vegetation in these seasons, were performed. Boundary conditions for the simulations were taken from the experiment conducted at Fazenda Água Limpa, University of Brasilia, in the two vegetation covers. Mean velocity values at 100m height were calculated for the two covers and periods considered. Note that in the Cerrado the values for dry and wet seasons, 6.92 m/s and 6.84 m/s, respectively, are very close with a slightly higher average for the dry period, approximately 1%. For Eucalyptus, on the other hand, a more pronounced difference, 4.38 m/s and 5.49 m/s, close to 20%, were found. Comparing now the effects of vegetation cover, it was verified that during the humid period, the speed at 100m is almost 20% higher in the Cerrado. In the dry period, this difference reaches more than 35%. This results highlight the importance of considering vegetation cover when determining wind energy potential.*

Keywords: *wind energy, canopy flow, atmospheric boundary layer*

1. INTRODUCTION

Wind turbines, because of their size, are invariably embedded in a region of the atmosphere called the Atmospheric Boundary Layer (ABL). The ABL can be defined as the part of the troposphere that is directly influenced by the presence of the Earth's surface and responds to surface forcings on time scales of one hour or less (Stull, 1988). The ABL, therefore, comprises the lowermost layers of the troposphere. However, its vertical extent is on the order of 1km during the day. Therefore, since modern wind turbines have blade tip heights of close to 200m, they are subject to the dominant processes in the ABL.

The relevance goes beyond the direct effect of surface roughness, but also includes the thermal properties of the surface, such as thermal conductivity, albedo and stomatal conductance. All these physical properties have indirect interference on wind generation to the extent that they control the partitioning of the solar radiation incident on the surface into sensible and latent heat (Bowen's ratio) exchanged between, and therefore influence the wind speed and turbulence characteristics during the daily evolution of the ABL.

Given the complexity of the phenomena and multiplicity of the parameters, for a better understanding of these influences in various situations, modeling is necessary. For convective ABL evolution, layer models (Driedonks, 1982; Tennekes and Driedonks, 1981) are the most used. However, in the case at hand, the momentum and energy fluxes near the surface, in the so-called surface layer of the ABL, are relevant thus requiring specific modeling.

There is a hierarchy of models that allows simulation of the flow in this region of the domain. Some, more sophisticated models, explicitly resolve the larger scales of turbulence in the ABL, known as Large Eddy Simulation

(LES). Nonetheless, LES models are, by nature, 3-D and transient, requiring computational resources and time incompatible with the long-term multiple-situation simulations. On the other hand, other models are less computationally demanding and fast runs and still provide physically sound results, such as 1-D Reynolds Average Navier-Stokes (RANS) models, in which a horizontally homogeneous surface is assumed, and turbulence effects are estimated in an integrated manner at all scales of the flow. However, these require the establishment of empirical parameters that are subject to validation. Here, the later approach is adopted, which seems to represent a good compromise between results and computational demand, as it is well accepted in wind energy community (Morales Garza et al., 2019) in which parameters found in the literature for two vegetation covers, namely native Cerrado and Eucalyptus plantation are considered to better understand the influence of this properties in wind-power potential. The choice of these vegetation covers is appropriate for this study not only because they are common in the Centro-Oeste region of Brasil, but also due to their very different canopy properties, both eco-physiological and architectural.

2. METHODOLOGY

Canopy elements, such as foliage, branches and trunks, act as sources (or sinks), both for momentum and scalars that include, for example, absorption and emission of CO2 by photosynthesis and respiration, respectively, transpiration by individual leaves via stomatal pores, sources or sinks of heat due to interception of solar radiation and emission of thermal radiation by canopy elements, among others (Siqueira et al., 2011). These elements vary considerably in space, with distributions that are function of the type of vegetation, as can be visually seen in Figure 1.

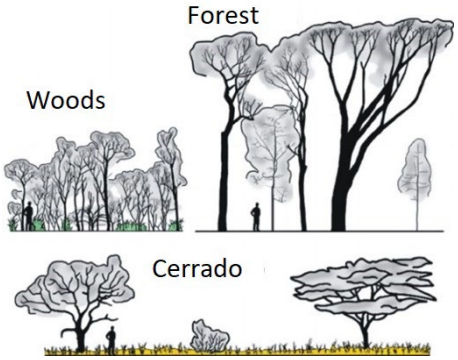

Figure 1: Canopy structure for different types of vegetation

Since these momentum and scalars sources and sinks are spatially distributed over several length scales, and, given the impossibility of solving all these scales, it becomes necessary to solve double-averaged (both spatially and temporally) constitutive equations (Raupach and Shaw, 1982). This averaging procedure follows the conventional Reynolds method, with the addition of averaging applied over thin horizontal layers that include a significant number of canopy elements, making the problem horizontally homogeneous and therefore one-dimensional. This fact allows estimates of the velocity fields and scalars compatible with the scales of interest. The effects of these canopy elements on scalar flow must be modeled through a drag force or rate of emission or absorption of scalars, which are often biologically active, such as latent heat, and, indirectly, sensible heat, and CO_2. In addition, thermal buoyancy imposes coupling at different intensities depending on synoptic conditions between the velocity field and that of scalars.

A natural starting point for a development in the direction of the understanding canopy physical and ecophysiological properties effects in wind energy potential is to first consider solving the flow in the regions under direct canopy influence, also called canopy sub-layer, where classical boundary layer theories fail due to their proximity to the source of the variable (Raupach and Shaw, 1982). Boudreault et al (2014) already showed the relevance of proper description of canopy structure properties in wind, however their work did not look at different vegetation cover and seasonal variability, the focus of this work. The canopy sublayer can extend vertically for 2 to 3 canopy heights but controls the entire ABL as surface fluxes determine its evolution throughout the day. In this region, 1st order turbulence models, where a direct relationship between flux and gradient is assumed, are not suitable (Raupach and Shaw, 1982). Therefore, here, a 2nd order model, presented below, is used, in which Reynolds stresses are solved explicitly by their transport equations.

It is important to mention that, in the ABL as whole, the turbulence is mostly thermally driven, conditions in which unstable or stable prevail in opposite of neutral conditions assumed here by solving momentum equation only. However, since this work deals with the lower part of ABL, it is not uncommon that mechanically-produced turbulence is more relevant, given that the canopy sublayer is often lower than the Obukhov length. Additionally, understanding the role of vegetation morphology in determining the wind energy potential is a first step to deconvolve the thermal from mechanical effects of vegetation in wind power generation.

2.1 Numerical Model

For an extensive and horizontally homogeneous canopy, the one-dimensional (time-averaged and horizontal) conservation equation for the momentum in the longitudinal direction (*x*, aligned with flow; *z* vertical) in a canopy is given by (Thom, 1971):

$$\frac{\partial \overline{u}}{\partial t} = -\frac{\partial \overline{u'w'}}{\partial z} - F_{d,c}, \tag{1}$$

where *u* and *w* are the longitudinal and vertical components of velocity, respectively, $F_{d,c} = C_d a \overline{u}|\overline{u}|$ is the drag force of the leaves in the flow, $a(z)$ is the leaf area density, C_d is the drag coefficient for the leaves, overbar denotes the temporal and horizontal averaging operator, and the superscript line represents excursions from this mean (Raupach and Shaw, 1982). The canopy turbulence model used here is based on 2nd order closure principles, in which transport equations for turbulent flows are derived and the turbulent kinetic energy (TKE) is decomposed into two band frequencies, namely low frequency "turbulent shear kinetic energy" (SKE) and high frequency "wake kinetic energy" (WKE) as discussed in J. D. Wilson, (1988) and Katul and Chang (1999). The canopy generated WKE was included to account for the deviation (or short-circuiting) of the usual turbulence energy cascade due to the intervention of drag elements (Cava and Katul, 2007; Poggi et al., 2004, 2008; Poggi and Katul, 2006). The conversion from SKE (SKE is denoted in the equations as k) to WKE is modeled as an additional dissipation term in k equation. No transport equation for WKE is needed because its feedback to SKE is considered minimal (J. D. Wilson, 1988). The transport equation for the tangential stress and the normal stress of the low frequency band (SKE band) is given by:

$$\frac{\partial \overline{u_i' u_j'}}{\partial t} = P_{ij} + R_{ij} + T_{ij} - \varepsilon_{ij}, \tag{2}$$

Here tensor notation is used where subscripts (*i,j*) refer to orthogonal coordinates, *P* is the production term, *R* is the redistribution term, *T* is the turbulent transport term, and ε is the dissipation term. The components of *P*, *R*, and *T* are obtained by applying the Reynolds average operator to the instantaneous momentum equations, shown below:

$$P_{xx} = -2\overline{u'w'}\frac{\partial \overline{u}}{\partial z};\ P_{yy} = P_{zz} = 0;\ P_{xz} = -\overline{w'w'}\frac{\partial \overline{u}}{\partial z}, \tag{3}$$

$$R_{ij} = \overline{\frac{p'}{\rho_0}\left(\frac{\partial u_i'}{\partial x_j} + \frac{\partial u_j'}{\partial x_i}\right)}, \tag{4}$$

$$T_{ij} = -\frac{\partial\left(\overline{w'u_i'u_j'}\right)}{\partial z}, \tag{5}$$

The *R* and $\overline{w'u_i'u_j'}$ terms require parameterization. In this work the parameterization suggested by J. D. Wilson (1988) was adopted and consists of:

$$R_{ij} = R_{ij,1} + R_{ij,2} + R'_{ij,1}, \tag{6}$$

$$R_{ij,1} = -\frac{c_1\varepsilon}{k}\left(\overline{u_i'u_j'} - \frac{2}{3}\delta_{ij}k\right), \tag{7}$$

$$R_{ij,2} = -c_2\left(P_{ij} - \frac{2}{3}P\delta_{ij}\right), \tag{8}$$

$$R'_{ij,1} = -\frac{c_1'\varepsilon}{k}\left(\overline{u_i'u_j'}n_k n_m \delta_{ij} - \frac{3}{2}\overline{u_k'u_i'}n_k n_j - \frac{3}{2}\overline{u_k'u_j'}n_k n_i\right) f\left(\frac{l}{z}\right), \tag{9}$$

$$\overline{u_i'u_j'u_k'} = c_s\frac{k}{\varepsilon}\left(\overline{u_i'u_l'}\frac{\partial \overline{u_j'u_k'}}{\partial x_l} + \overline{u_j'u_l'}\frac{\partial \overline{u_i'u_k'}}{\partial x_l} + \overline{u_k'u_l'}\frac{\partial \overline{u_i'u_j'}}{\partial x_l}\right), \tag{10}$$

The full description of the terms and their arguments are presented by J. D. Wilson, (1988). It is worth mentioning that the function $f\left(\frac{l}{z}\right)$ represents a function of proximity to the wall (soil in this case), given by:

$$f\left(\frac{l}{z}\right) = \frac{c_{flz}}{z}\left(\frac{k^{\frac{3}{2}}}{\varepsilon}\right), \tag{11}$$

with , $c_{flz} = \frac{1}{\left(k_v k^{\frac{3}{2}}\right)}$ where k_v is the Von Karman constant. The triple correlation term (9) is also modified to account for the presence of the canopy through the constant c_s:

$$c_s = c_{s0}\left(1 + LAI \sin\left(\frac{\pi z}{h}\right)\right), \tag{12}$$

where LAI represents the leaf area index defined by $LAI = \int_0^h a(z)\, dz$, and h is the canopy height.

The dissipation rate is decomposed into two contributions given by J. D. Wilson (1988):

$$\varepsilon_{ij} = \frac{2}{3}\varepsilon\delta_{ij} + \left(2C_d a\overline{u}\overline{u_i'u_j'}\delta_{ij} + 2C_d a\overline{u}\overline{u_i'u_j'}\delta_{i1}\delta_{j1}\right), \tag{13}$$

without implicit summation over repeated rates. Here, ε is the viscous dissipation rate and the term in parentheses represents the additional SKE to WKE transformation. Unlike previous closure models (Katul and Chang, 1999; J. D. Wilson, 1988), a real transport equation for ε was used for better representation of the dissipation terms. This equation is given by (Hanjalić and Launder, 1972; Katul et al., 2004):

$$\frac{\partial \varepsilon}{\partial t} = \frac{\partial}{\partial z}\left(c_{\varepsilon 3}\frac{k}{\varepsilon}\overline{w'^2}\frac{\partial \varepsilon}{\partial z}\right) + c_{\varepsilon 1}\frac{\varepsilon}{k}\frac{P_{ii}}{2} - c_{\varepsilon 2}\frac{\varepsilon^2}{k}, \tag{14}$$

where $c_{\varepsilon 3}$, $c_{\varepsilon 1}$ and $c_{\varepsilon 2}$ are model constants that can be determined using arguments presented in (Katul et al., 2004) and (Sanz, 2003). The equations can be normalized by the friction velocity ($u^* = \sqrt{-\overline{u'w'}(h)}$) because in the surface-layer flow variables scale consistently with it.

The model consists of solving the differential equations (1), (2) (for all components) and (14), together with the definition in Eq (13). However, they do not allow analytical solution and have to be solved numerically, by Computational Fluid Dynamics (CFD). As already mentioned, the horizontal homogeneity approximation, allows them to be discretized only in the vertical (1-D) direction resulting in vertical profiles of the calculated variables. The discretization adopted here was by finite volume technique.

3. RESULTS AND DISCUSSION

The model described in previous section was run for the two vegetative covers, Cerrado and Eucalyptus. Table 1 presents the values of the empirical constants used in the solution of the equations. The characteristics that differentiate the two vegetative covers in the simulations presented here are the canopy height, h, and the vertical distribution of leaf area density, $a(z)$. As typical for this region, seasonality is characterized by two very distinct periods, a wet season (from October to March) and a dry season (from April to September). Simulations were performed for each season and vegetation covers. Canopy height was assumed to be the same for both periods.

Table 1: Empirical constant values

c_1	c_2	c_1'	c_{s0}	$c_{\varepsilon 1}$	$c_{\varepsilon 2}$	$c_{\varepsilon 3}$	C_d
1.8	0.6	0.5	0.11	1.44	1.92	0.16	0.2

Table 2: Physical properties of the vegetation covers for the two periods considered.

Vegetation / Season	Cerrado			Eucalyptus		
	h [m]	IAF	a_Γ	h [m]	IAF	a_Γ
Humid	8	3.2	6	25	5.4	1.5
Dry	8	2.0	6	25	3.0	1.5

As the exact leaf vertical distribution has small impact on wind energy potential (Morales Garza, 2019), a generic functional form for leaf area density for both vegetation covers was adopted. The $a(z)$ profiles were generated by a probability density function Γ with shape parameter, a_Γ, specified for each cover, but scaled based on the LAI value, the

latter with specific values for each season of the year. The parameter a_I for each vegetation cover was chosen to translate the morphology of each vegetation, considering the vertical distribution of leaf area in the Cerrado more uniform than in the Eucalyptus, in which there is a greater concentration in the upper part of the canopy. Seasonal differences reflect the phenology of each vegetation, characterized by lower density in the dry season due to loss of dry leaves (Almeida et al., 2007; Lemos-Filho et al., 2010). Table 2 shows the values of these properties for each vegetation and Figure 2 shows the vertical distribution of leaf area and for the two periods of the year considered in the study.

The boundary conditions adopted in the simulations follow usual values of turbulent ABL, namely, $\frac{\overline{u'w'}}{u^{*2}} = -1$ (by definition), $\frac{\overline{u'u'}}{u^{*2}} = 2.4$, $\frac{\overline{v'v'}}{u^{*2}} = 1.95$, $\frac{\overline{w'w'}}{u^{*2}} = 1.25$ and $\frac{d\overline{u}}{dz} = \frac{u^*}{k_v z}$. The results of the velocity statistics normalized by u^* are presented in Figure 3. It is noticeable the difference in behavior between the two vegetations in the regions closer to the canopy. However, as one moves away from the canopy sublayer the behavior recovers what would be consistent with the inertial layer of the ABL, with mechanical source dominating turbulence generation with prevalence of the energy cascade. Nevertheless, given the different heights, the turbulence stabilizes at different values for different vegetation.

It is worth noting that there are practically no major differences between these statistics for the two periods. However, in absolute values there will be differences by the different u^*.

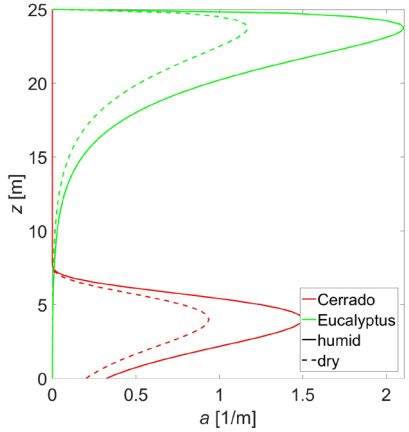

Figure 2: Vertical distribution of leaf area density for the two vegetation covers and seasons.

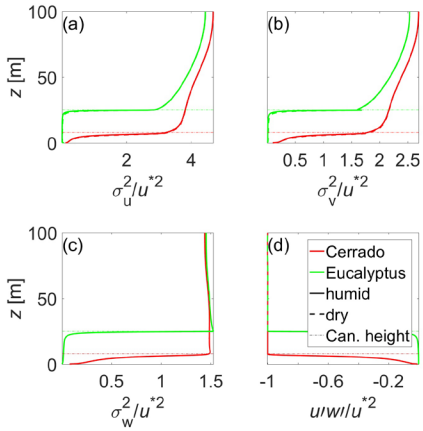

Figure 3: Simulated normalized velocity statistics for the two vegetations and periods of the year. (a) streamwise velocity variance, σ_u^2; (b) transversal velocity variance, σ_v^2; (c) vertical velocity variance, σ_w^2; (d) longitudinal-vertical velocity covariance, $u'w'$.

The simulated velocity profiles are shown in Figure 4. It is evident the influence of the physical properties of the vegetation cover on the longitudinal velocity due to differences in drag by the vegetation elements. As expected, both canopy height and leaf area density influence the wind speed at heights compatible with wind turbine operation. Canopy height has stronger relative impact due to the discrepancy in the zero-plane displacement. However, even though LAI effect is minor when compared to height, there are important differences between wet and dry period, which may result seasonality in wind power. . These factors can have a relevant impact on the wind potential available for a 100m high turbine, upper end of Figure 4.

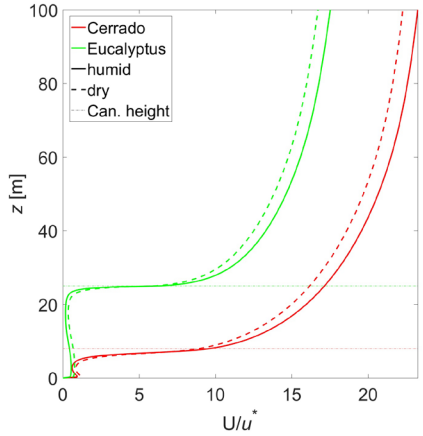

Figure 4: Simulated velocity profiles for the two vegetations and periods of the year.

As the simulation results are normalized by u^*, they do not inform the actual wind statistics. Therefore, for a more realistic evaluation of the sensitivity of the wind-energy potential to different covers, it is plotted in Figure 5 the daily evolution of wind speed and turbulent kinetic energy (k) at 100m height using the ensembled-averaged u^* for each half-hour of the two periods of the year studied. These two velocity statistics were chosen because they might have impact on wind power conversion. u^* data were collected with eddy-convariance towers, equipped with sonic anemometers, in each vegetation cover , Cerrado and Eucalyptus at Fazenda Água Limpa, a research facility maintained by University of Brasilia. For averaging purpose, the months of December/2014-January-February/2015, representative of wet season, and June-July-August/2015, representative of dry season, were considered. These periods are the ones that have best data quality of the eddy-covariance tower for the two vegetation covers. As expected, the Cerrado vegetation cover induces considerably higher velocities than the Eucalyptus. It is interesting to note, however, that the behavior is distinct between the two vegetation covers with respect to seasonality. While in the Cerrado the velocity values are higher in the dry season than in the wet season, the opposite is observed for the Eucalyptus area. It is worth mentioning is the differences in evolution during the day. In the dry season, there is a more pronounced peak around 10:00 am for both vegetation covers, a fact not observed in the wet season, which presents a more uniform distribution during the daytime period. Temporally, the behavior of k is similar to wind speed because both follow daily variation in u^*. However, given that k scales with the square of u^* and there are differences in σ_u^2 and σ_u^2 between the vegetations, model results suggests that Cerrado has far more pronounced seasonality in k then Eucalyptus. Some caution is necessary when analyzing night-time data, low u^* and negative heat fluxes. With the stable atmospheric conditions that are formed in the absence of solar radiation, there is suppression of turbulence, which reduces the coupling of the velocity profile with the surface. This fact limits the applicability of the model that may be underestimating the wind speed at 100m. In this case, the simultaneous calculation of velocity and energy may alleviate this deficiency of the model, which will be subject of future studies.

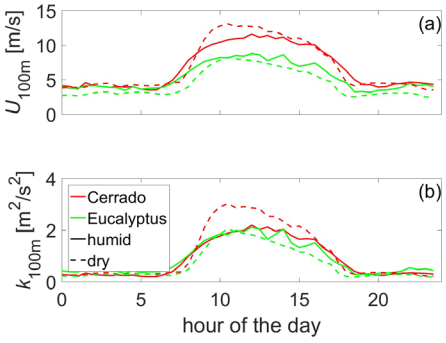

Figure 5: Daily wind speed evolution at 100m for the two vegetative covers and the two periods of the year.

Finally, it is important to evaluate the integrated value of the velocity over the entire period. Table 3 shows the values of the average velocity at 100m height for the two covers and periods considered. Note, that in the Cerrado a closer value between the two seasons of the year, with a slightly higher average in the dry period, approximately 1%. For Eucalyptus, a more pronounced difference is observed with the opposite behavior to the Cerrado, with a difference close to 20%.

Comparing now the effects of vegetation cover, it is verified that during the humid period, the speed at 100m is almost 20% higher in the Cerrado. In the dry period, this difference reaches more than 35%. As mentioned before, this behavior has its origin in two main factors, the lower LAI in the Cerrado at any time of the year and the higher height of the Eucalyptus itself.

Table 3: Average velocity at 100 m height for the two vegetation covers and seasons.

Vegetation / Season	Cerrado	Eucalyptus
	Mean wind speed at 100m	Mean wind speed at 100m
Humid	6.84 [m/s]	5.50 [m/s]
Dry	6.92 [m/s]	4.38 [m/s]

4. CONCLUSIONS

Using a 2nd order Reynolds Averaged model simulation of canopy were performed for two different vegetation covers, Cerrado and Eucalyptus plantation, for two distinct seasons, wet and dry, typical for the Centro-Oeste region of Brazil. The goal was to better understand effects of canopy structure on wind power potential for wind energy applications. Simulations results highlight the importance of considering the canopy architecture in wind power projects given marked differences in the seasonal behavior when Cerrado and Eucalyptus are compared.

It is worth stressing that these findings are preliminary as the role of thermal source turbulence generation is not being taken into account. For situations where u* is low, this may be an important factor to consider and may change some of values presented. However, it is not foreseen that these conclusions would not hold.

5. ACKNOWLEDGEMENTS

This research was based upon a R&D Project from ANEEL - National Agency, "Otimização do modelo meteorológico BRAMS, com validação experimental, para subsidiar aperfeiçoamentos de modelagens em sistemas eólicos" – PD-0394-1709/2017, supported by Eletrobras Furnas with University of Brasilia cooperation

6. REFERENCES

Almeida, J. C. R. de, Laclau, J.-P., Gonçalves, J. L. de M., and Rojas, J. S. D., 2007. Índice de área foliar de Eucalyptus grandis em resposta à adubação com potássio e sódio. Anais Do I Seminário de Recursos Hídricos Da Bacia Hidrográfica Do Paraíba Do Sul, 1–7.

Boudreault, L. É., Bechmann, A., Sørensen, N. N., Sogachev, A., and Dellwik, E. 2014. Canopy structure effects on the wind at a complex forested site. In Journal of physics: Conference series (Vol. 524, No. 1, p. 012112). IOP Publishing.

Cava, D., and Katul, G. G., 2007. Spectral Short-circuiting and Wake Production within the Canopy Trunk Space of an Alpine Hardwood Forest. Boundary-Layer Meteorology 2007 126:3, 126(3), 415–431. https://doi.org/10.1007/S10546-007-9246-X

Driedonks, A. G. M., 1982. Models and observations of the growth of the atmospheric boundary layer. Boundary-Layer Meteorology, 23(3), 283–306. https://doi.org/10.1007/BF00121117

Hanjalić, K., and Launder, B. E., 1972. A Reynolds stress model of turbulence and its application to thin shear flows. Journal of Fluid Mechanics, 52(4), 609–638. https://doi.org/10.1017/S002211207200268X

Katul, G. G., and Chang, W., 1999. Principal Length Scales in Second-Order Closure Models for Canopy Turbulence. Journal of Applied Meteorology and Climatology, 38(11), 1631–1643. https://doi.org/10.1175/1520-0450(1999)038

Katul, G. G., Mahrt, L., Poggi, D., and Sanz, C., 2004. ONE- and TWO-Equation Models for Canopy Turbulence. Boundary-Layer Meteorology 2004 113:1, 113(1), 81–109. https://doi.org/10.1023/B:BOUN.0000037333.48760.E5

Lemos-Filho, J. P., Barros, C. F. A., Dantas, G. P. M., Dias, L. G., and Mendes, R. S., 2010. Spatial and temporal variability of canopy cover and understory light in a Cerrado of Southern Brazil. Brazilian Journal of Biology, 70(1), 19–24. https://doi.org/10.1590/S1519-69842010000100005

Morales Garza, V. G., Sumner, J., Nathan, J., and Masson, C. 2019. Evaluating the Accuracy of RANS Wind Flow Modeling Over Forested Terrain—Part 1: Canopy Model Validation. Journal of Solar Energy Engineering, 141(4), 041009.

Poggi, D., and Katul, G. G., 2006. Two-Dimensional Scalar Spectra in the Deeper Layers of a Dense and Uniform Model Canopy. Boundary-Layer Meteorology 2006 121:2, 121(2), 267–281. https://doi.org/10.1007/S10546-006-9075-3

Poggi, D., Katul, G. G., and Albertson, J. D., 2004. Momentum transfer and turbulent kinetic energy budgets within a dense model canopy. Boundary-Layer Meteorology, 111(3), 589–614. https://doi.org/10.1023/B:BOUN.0000016502.52590.AF

Poggi, D., Katul, G. G., and Cassiani, M., 2008. On the anomalous behavior of the Lagrangian structure function similarity constant inside dense canopies. Atmospheric Environment, 42(18), 4212–4231. https://doi.org/10.1016/J.ATMOSENV.2008.01.020

Raupach, M. R., and Shaw, R. H., 1982. Averaging procedures for flow within vegetation canopies. Boundary-Layer Meteorology 1982 22:1, 22(1), 79–90. https://doi.org/10.1007/BF00128057

Siqueira, M. B., Katul, G. G., Tanny, J., Siqueira, M. B., Katul, G. G., and Tanny, J., 2011. The Effect of the Screen on the Mass, Momentum, and Energy Exchange Rates of a Uniform Crop Situated in an Extensive Screenhouse. Boundary-Layer Meteorology 2011 142:3, 142(3), 339–363. https://doi.org/10.1007/S10546-011-9682-5

Stull, R., 1988. An introduction to boundary layer meteorology.

Tennekes, H., and Driedonks, A. G. M., 1981. Basic entrainment equations for the atmospheric boundary layer. Boundary-Layer Meteorology, 20(4), 515–531. https://doi.org/10.1007/BF00122299

Wilson, J. D., 1988. A second-order closure model for flow through vegetation. Boundary-Layer Meteorology, 42(4), 371–392. https://doi.org/10.1007/BF00121591

7. RESPONSIBILITY NOTICE

The authors are the only responsible for the printed material included in this paper.